

General Disclaimer

One or more of the Following Statements may affect this Document

- This document has been reproduced from the best copy furnished by the organizational source. It is being released in the interest of making available as much information as possible.
- This document may contain data, which exceeds the sheet parameters. It was furnished in this condition by the organizational source and is the best copy available.
- This document may contain tone-on-tone or color graphs, charts and/or pictures, which have been reproduced in black and white.
- This document is paginated as submitted by the original source.
- Portions of this document are not fully legible due to the historical nature of some of the material. However, it is the best reproduction available from the original submission.

NASA TM X-71150

REANALYSIS OF THE APOLLO COSMIC GAMMA-RAY SPECTRUM IN THE 0.3- TO 10-MeV ENERGY REGION

(NASA-TM-X-71150) REANALYSIS OF THE APOLLO
COSMIC GAMMA-RAY SPECTRUM IN THE 0.3 TO 10
MeV ENERGY REGION (NASA) 36 p HC \$4.00

N76-28148

CSCI 03E

Unclas

G3/93

45871

JUNE 1976

GSFC

— GODDARD SPACE FLIGHT CENTER —
GREENBELT, MARYLAND

Reanalysis of the Apollo Cosmic Gamma-ray Spectrum
in the 0.3- to 10-MeV Energy Region

J. I. Trombka
NASA/Goddard Space Flight Center
Greenbelt, Maryland 20771

C. S. Dyer
University of Maryland
College Park, Maryland 20742

L. G. Evans and M. J. Bielefeld
Computer Sciences Corporation
Silver Spring, Maryland 20910

S. M. Seltzer
National Bureau of Standards
Gaithersburg, Maryland 20760

and

A. E. Metzger
Jet Propulsion Laboratory
Pasadena, California

ABSTRACT

Additional data obtained from the Apollo-16 and -17 missions, together with collateral calculations on background radiation effects, have enabled an improved subtraction of unwanted backgrounds from the diffuse cosmic gamma-ray data previously reported from Apollo-15. As a result, the 1- to 10-MeV spectrum is lowered significantly and connects smoothly with recent data at other energies. The inflection reported previously is much less pronounced and has no more than a $1.5\text{-}\sigma$ significance. Sky occultation by the Apollo-16 spacecraft shows the bulk of the 0.3- to 1-MeV radiation to be diffuse. The analysis of spurious backgrounds points to important improvements for future experiments designed for this spectral region.

Subject headings: gamma rays -- celestial diffuse radiation

I. INTRODUCTION

The results of an analysis of the measurement of the cosmic gamma-ray spectrum in the range from 0.3 to 27 MeV obtained on Apollo-15 were reported earlier (Trombka et al., 1973). Since that time, further in-flight data obtained from Apollo-16 and data from an identical crystal carried and returned on Apollo-17 (Dyer et al., 1975a) and Apollo-Soyuz (Trombka et al., 1976) have been analyzed and show additional background effects. Furthermore, an improved calculation of spallation has been developed (Dyer et al., 1975a). The purpose of this paper is to reassess the previous results and present our best estimate of the differential energy spectrum of the total cosmic gamma-ray flux in the energy region from 0.3 to 10 MeV.

A number of features which had earlier presented difficulties has now been explained. An enhanced counting rate of approximately 15 percent from Apollo-16 compared with Apollo-15 can be explained by bremsstrahlung effects due to electrons of energy 1 to 20 MeV. A high level of activation observed in a crystal returned on the Apollo-17 mission has been attributed to a significant flux of secondary neutrons produced in the heavy spacecraft. In addition, a flux of discrete lines has been carefully subtracted. These are attributable to nuclear interactions in local materials. Finally, correction has been made for the attenuation and energy degradation of the incident gamma-ray flux by the material surrounding the detector.

The shape of the cosmic gamma-ray spectrum is of great interest in discussions regarding the astrophysical and cosmological origin of the radiation. These results are also significant because of the considerable disparity in the results presented to date with respect to the nature and magnitude of the observed spectrum. The reanalysis has provided a greater understanding of backgrounds affecting such measurements and should also aid in the design and analysis of future experiments.

II. INSTRUMENTATION

The Apollo gamma-ray spectrometer comprised a 7.0-cm diameter by 7.0-cm long NaI(Tl) scintillation crystal coupled to a 7.6-cm photomultiplier, a plastic mantle for the anticoincidence rejection of charged particles, and an analog-to-digital (A/D) converter giving 511 channels of analysis. The 1-cm thick plastic scintillator shield surrounded the central crystal completely except at the photomultiplier end. The anticoincidence system had a threshold of about 1.0 MeV for generating an anticoincidence pulse when interaction occurred in the most optically unfavorable location. The shield rate, the coincidence rate, and the live time were transmitted every 0.328 s. Those central detector events, having no shield anticoincidence, were analyzed by pulse-height into 511 channels and were transmitted at a maximum rate of 370 counts s^{-1} .

The spectrometer and associated electronics were enclosed in a thermal shield and mounted on a boom which could be extended from one side of the Apollo service module. The deployment of the detector was under astronaut

control. In its fully deployed position the detector was 7.6 m from the spacecraft surface. Intermediate distances were also achieved by using stopwatch timing during deployment. The components carried on the boom shielded the crystal by $\sim 7.6 \text{ g cm}^{-2}$ averaged over all directions except in the boom direction where $\sim 20 \text{ g cm}^{-2}$ was presented. Details of the spectrometer design and operation can be found in Harrington et al. (1974).

III. BACKGROUND CORRECTIONS

In order to infer the shape and magnitude of the cosmic gamma-ray spectrum from the observed energy-loss spectrum, unwanted background components must be subtracted. A brief description of those identified in the Apollo experiment is given below. Because of their importance to medium energy gamma-ray astronomy, a fuller description of their identification and computation is in preparation. Further details may be found in Dyer et al. (1975a and 1975b) and Trombka et al. (1976).

(a) Direct Charged-particle Detector Counts

An active charged-particle shield was used to eliminate this component of the background. The effect of the active shield was described in detail in Trombka et al. (1973). In the region up to 10 MeV, the charged-particle interference is negligible compared with the magnitude of the cosmic gamma-ray spectrum. However, above about 12 MeV, the anticoincidence rejection efficiency has now been found to be insufficient to adequately remove the charged-particle background. Thus, our present analysis is limited to the energy region below 10 MeV.

Although the shield was found to be highly efficient at all positions when mapped with a beta source, the ~0.5-percent inefficiency could result from occasional unfavorable particle paths from which insufficient light is transmitted to exceed the shield threshold. Alternatively, the open end of the plastic shield may allow a small fraction of the charged-particle flux to stop in the crystal without triggering an anticoincidence pulse.

(b) Natural Radioactivity

The magnitude of the natural radioactivity in the spacecraft was determined by preflight surveys of the Apollo-15 and Apollo-16 Command and Service Modules. The results of the survey can be found in Metzger and Trombka (1972). The contribution of this source is much lower than the cosmic-ray-induced radiation and is included as part of the spacecraft component, which is described in the following paragraph. In addition, a small trace of ^{40}K was found in the glass used in the seal between the NaI(Tl) crystal and photomultiplier tube. The line from this source is included in the removal of local radioactivity, as described in paragraph (g).

(c) Spacecraft Component

Cosmic-ray primary and secondary interactions in the spacecraft and the natural radioactivity of spacecraft materials provide a major background component. This component can be extracted from in-flight data obtained at various boom positions on both Apollo-15 and -16. The expected dependence of the spacecraft component on boom extension was calculated theoretically as a

function of energy assuming the spacecraft to be a cylinder of aluminum in which the source of gamma radiation is uniformly distributed (Seltzer, 1976). Two important results were obtained from these calculations. First, the variation of the spacecraft component of the gamma-ray flux with distance is nearly independent of energy for the boom extensions and energies applicable to the Apollo missions, a fact which eliminated the need to make any a priori assumptions about the spectral shape of the spacecraft component. Secondly, the boom-length dependence differs by as much as 55 percent from a simple inverse-square law over the range of the Apollo boom extensions due to the size of the spacecraft.

A least-squares analysis was performed on the channel-by-channel count rate obtained at various boom positions between 0.6 and 7.6 m, assuming that the cosmic gamma-ray flux, plus the background due to effects in the local matter, are independent of boom position while the spacecraft component varies as calculated. The spectral shape and magnitude of the spacecraft contribution at 7.6 m is shown in Figure 1 for Apollo-16. A 0.511-MeV line occurs in both the spacecraft and the local-plus-cosmic components, whereas the lines at 0.65 and 1.4 MeV seem to be associated with the local-plus-cosmic component. The spacecraft component is dominated by an electron-photon cascade continuum with the associated annihilation line, although discrete lines due to nuclear reactions are also present. The discrete lines in the local-plus-cosmic component can be ascribed to activation in the detector and in materials surrounding

the detector. These components will be considered later. The spacecraft contributions obtained for Apollo-15 and -16 agree to within three percent.

(d) Electron Bremsstrahlung

The pulse-height spectra measured on Apollo-15 and Apollo-16 are compared in Figure 1 and show a 15-percent difference. The calculation described above indicated that the enhancement in the observed Apollo-16 spectrum was associated with the local-plus-cosmic component. A number of possible contributing sources was investigated and the following was the only successful explanation of the magnitude and spectral shape of the difference between the two observations.

At the time of the Apollo-16 mission (April 1972), there was a quiet-time, low-energy electron increase, possibly of Jovian origin (Teegarden et al., 1974). Data obtained from the IMP-5 detector (Van Hollebeke, private communication) shows the 3- to 12-MeV electron flux to be enhanced by a factor of 1.9 ± 0.2 between the times of the Apollo-15 and -16 missions. Using a power law with a spectral index of -1.75 for the description of the differential electron energy spectrum (Teegarden et al., 1974) and a thickness of 7.6 g cm^{-2} of aluminum surrounding the detector, the magnitude and shape of the energy-loss spectrum due to electron bremsstrahlung were obtained by means of an approximate calculation based on the results of Berger and Seltzer (1968). The calculated spectrum matches the Apollo-16 increase relative to Apollo-15 to within 10 percent over the entire 0.3- to 10-MeV energy range.

The smoothed difference between the Apollo-15 and Apollo-16 data was used directly with the observed electron increase to calculate the bremsstrahlung contribution for each mission, and the result for Apollo-16 is plotted in Figure 1. Identification of this component provides a major difference between this analysis and that presented previously (Trombka et al., 1973).

(e) Cosmic-ray-induced Radioactivity in the Central Crystal

One of the major uncertainties identified in our previous analysis was lack of knowledge of the spallation-induced activity. To obtain the previous results, the estimates of Dyer et al. (1972) and Fishman (1972) were somewhat arbitrarily halved in order to obtain a cosmic gamma-ray spectrum without major discontinuities. These estimates considered only isotopes of half-life greater than 1 min for which energy losses in excess of 4 MeV are negligible. However, in the Apollo detector, all half-lives greater than 10 μ s can contribute. Light fragments such as ^8Li , ^9Li , ^{12}B , and ^{16}N , which have half-lives in the range milliseconds to seconds, can deposit up to 15 MeV in the crystal and have a total production cross section of about 40 mb in NaI according to the estimates of Silberberg and Tsao (1973).

Since our original analysis, a computation scheme has been established which uses the best available nuclear data to calculate decay rates and energy-loss spectra of radioactive nuclides inside detector materials (Dyer et al., 1975a; Seltzer, 1975). So far, response functions have been computed for 70 radioactive nuclides for which the cross sections exceed 10 mb for 1-GeV

proton irradiation of NaI. This list is sufficient to predict only about one-half of the cosmic-ray-produced radioactivity. Allowance has been made for the contribution of missing species by doubling the continuum below 4 MeV. Response functions have also been computed for all significant light fragments and their contributions have been calculated. Clearly, the exact contributions of missing species and light fragments require further experimental investigation.

The results of the new calculations of the background due to cosmic-ray-induced activity in the detector for Apollo-16 are shown in Figure 1.

At energies below 4 MeV, the new estimate of this spallation component is about 2/3 the level calculated by Dyer et al. (1972). Most of this change, in fact, results from a corrected value for the average path length of isotropic cosmic rays in the crystal. Above 4 MeV, inclusion of a hard component resulting from light fragments accounts for part of the difference between the present analysis and our earlier calculation of the cosmic gamma-ray spectrum.

(f) Secondary Neutron-induced Radioactivity in the Central Crystal

Results of measurement of induced activity in identical crystals after return from the Apollo-17 and Apollo-Soyuz missions (Dyer et al., 1975a; Trombka et al., 1976) indicate a significant level of neutron activation of the central detector. Activation effects due to passage through the radiation belts on launch were considered in this analysis and found to be negligible. Using the observed levels of the secondary neutron products from the Apollo-17

returned crystal together with the boom extension history, the decay rates of species with half-lives down to several hours were calculated for the in-flight measurements. These give the energy-loss spectrum shown in Figure 1.

The correctness of the extrapolated neutron-induced spectrum can be inferred from the successful removal of the 600- to 700-keV feature on subtraction from the observed energy-loss spectrum. This feature is due to ^{126}I and ^{124}I . The level of ^{24}Na activation is confirmed from a 15-hour half-life decay component observed after boom extension from the stowed position. The in-flight data were selected so that there was no significant contribution from shorter half-lives produced by secondary neutrons which would have been missed in the returned crystal.

(g) Radioactivity in Materials Surrounding the Detector

The remaining background due to natural and induced radioactivity in materials surrounding the detector produces discrete lines and was removed during the spectral unfolding process as discussed in the next section. Any cosmic lines were also removed in this procedure.

Figure 2 shows the magnitude and spectral shape of the separated discrete line contribution in energy-loss space.

Table 1 gives the derived photon intensities for the discrete lines identified in the data. Differences in the intensities between Apollo-15 and Apollo-16 are not significant and are indicative of the errors. These lines are most likely ascribable to nuclear interactions in the steel, aluminum, and plastic surrounding the detectors. The annihilation line at 0.511 MeV is approximately a factor

80 more intense than the cosmic intensity measured by Haymes et al. (1975), while lines at 1.6 MeV and 4.4 MeV are respectively factors of 5 and 2-to-3 more intense than features reported at approximately these energies by the same group (Hall et al., 1975).

While it is possible that the carbon line at 4.43 MeV represents a cosmic nuclear gamma-ray line, we feel it is much more likely to be of local origin. In view of the intensity of these gamma-ray lines, which are produced locally in materials common to all detector systems, it is clear that considerable caution must be exercised in ascribing to them a cosmic origin.

(h) Summary

The contributions of the various background components to the measured energy-loss spectra for Apollo-15 and Apollo-16 are presented in tabular form for a number of energy intervals in Table 2.

IV. DETERMINATION OF EQUIVALENT PHOTON SPECTRUM

(a) Unfolding Procedure

The measured energy-loss spectrum is not in one-to-one correspondence with the photon spectrum, but must be unfolded using the response functions describing the interaction of incident photons with the detector. A weighted least-squares matrix inversion method, which has been developed to perform this transformation, is described by Trombka and Schmadebeck (1968). The basis of the method is that the energy-loss spectrum p_i can be related to the

equivalent photon spectrum E_j as follows:

$$\rho_i \approx \sum_j E_j S_{ij} \quad (1)$$

where

ρ_i = the observed number of energy losses in the energy interval Δ_i about i ,

E_j = the number of incident photons in energy interval Δ_j about j , and

S_{ij} = the detector response as a function of i and j .

Information theory shows that equation 1 may be used to describe a continuous distribution if S_{ij} is chosen such that the discrete set of j 's be separated by no more than one-half the resolution for the given energy under consideration. The intervals of i are set by the A/D converter used and must also be less than half the resolution width. Because of these requirements, the measured energy-loss spectrum must be an overdetermined system with respect to the j energy intervals. Thus, equation 1 must be solved for E_j (the equivalent photon spectrum) utilizing a method such as least-squares analysis. The solution obtained can be written in matrix form as follows:

$$E = (\tilde{S}^T S)^{-1} \tilde{S}^T \rho, \quad (2)$$

where

E = the vector describing the equivalent photon energy spectrum,

S = the $m \times n$ matrix of the detector response function,

\tilde{S} = the transpose of S ,

ω = the diagonal matrix of the weighting function for each of the i intervals. (In terms of our measurement and error analysis procedure $\omega_i = 1/\sigma_i^2$ where σ_i^2 is the variance of the measured energy-loss spectrum), and

ρ = the vector of the energy-loss spectrum to be transformed.

The detector response function (S matrix) depends on the characteristics of the detector and, for non-spherical detectors, on the angular distribution of the incident gamma-ray flux. The extensive stochastic calculations previously done for the response of a 3-by-3-in. NaI detector (Berger and Saltzer, 1972) were repeated for the 7-by-7-cm Apollo detector. The results, adjusted to account for an isotropic photon flux simply attenuated by the average 7.6 g cm^{-2} of aluminum surrounding the crystal, were cast in a parameterized form to facilitate the interpolation necessary to construct the S matrix. The S matrix so obtained is not only used in the unfolding, equation 2, but also provides, via the simple matrix multiplication of equation 1, for the rapid refolding of any incident energy distribution. This feature was particularly useful in the iterative process outlined below.

When the incident spectrum is a mixture of a continuum component with a discrete-line component, the transformation obtained using equation 2 will contain discontinuities or oscillations in those regions where there are discrete lines. In order to separate the two components, the derived distribution was

smoothed through the discontinuities to give a first estimate of the photon continuum, which was then transformed through equation 1 to yield the equivalent energy-loss spectrum. This was then subtracted from the total, and the lines were identified by peak searching and their intensities determined by using the transformation (equation 2) to photon space. Transforming the line components back to energy-loss space and subtracting from the original data gave a second estimate of the continuum. This was then inverted to photon space, smoothed and subtracted, and the process repeated, until after two or three iterations, no significant change occurred in the two components.

The discrete line background obtained by this method is shown in Figure 2. The points represent the difference between the final smoothed continuum and the original data and the solid line is the unfolded spectrum of discrete lines. In Figure 3, the points represent the final continuum portion of the data and the solid line is the energy-loss transformation of the final continuum-photon component of the cosmic gamma-ray flux.

(b) Degradation of the Photon Spectrum by the Material Surrounding the Detector

The simple attenuation factor, incorporated in the response matrix, is the probability that an incident photon is transmitted with no change in energy by the $\sim 7.6 \text{ g cm}^2$ of aluminum surrounding the central crystal, but it does not account for the photon being transmitted with its energy reduced by scattering events. Thus, the unfolded spectrum is not only the cosmic gamma-ray

spectrum, but also includes a scattered component. The scattered component, characterized by a large buildup of low-energy photons, depends on the shape of the incident primary gamma-ray spectrum and the details of the complex geometry of material around the detector. However, correction factors in the form of the ratio of primary to total photons were estimated for appropriate power-law primary spectra using results of photon-transport calculations and were used to transform the unfolded spectrum to the cosmic gamma-ray continuum spectrum. As expected, the corrections are large in the low-energy region, the factors used being, for example, 0.38 ± 0.13 , 0.58 ± 0.13 , 0.80 ± 0.08 , and 0.96 ± 0.02 at 0.3, 0.6, 1.5, and 10.0 MeV, respectively.

(c) Error Analysis

The least-squares analysis can also be used to determine the standard deviation in the derivation of the equivalent photon spectrum. If the weighting function ω used in equation 2 is equal to the inverse of the variance for each energy-loss interval (channel), then each diagonal element of the $(\tilde{S} \omega S)^{-1}$ matrix will be equal to the variance in the derived photon intensity in that channel (Trombka and Schmadebeck, 1968). The variance calculated for each channel of the cosmic gamma-ray energy-loss spectrum, ρ_i , must include the error in each of the background components. After the spectrum is unfolded, the errors obtained must be compounded with the error involved in correcting for attenuation. Thus, the standard deviation quoted includes errors in the

magnitude of the background components, effects in performing the transformation from energy loss to photon space, and finally errors in correction for local mass absorption effects.

The error in the spacecraft component involves both statistical errors in fitting the channel-by-channel count rate to the geometric model and errors in the model. The former was obtained directly from the least-squares analysis and is typically approximately two percent. This was compounded with a generous estimate of the error in the geometric model obtained by determining the change in the magnitude of the spacecraft component that results from using a simple inverse-square law dependence instead of the corrected version for a homogeneous cylindrical distribution. This gives a combined uncertainty of 10 percent.

The variance in the bremsstrahlung estimate was obtained by compounding the statistical error in the difference spectrum with the error in the measured electron increase. The resulting channel-by-channel error in this component varies from 23 percent at low energies to 53 percent at 10 MeV for the Apollo-16 level.

Errors in the neutron activation estimate result from errors in the measurement of isotopes in the returned detector, and errors in extrapolating to the in-flight contribution. This is estimated to be approximately 60 percent, which is probably generous in view of the ability to fit in-flight line features.

The error in the cosmic-ray-induced spallation component is more subjective at this stage, pending a planned series of controlled monoenergetic irradiations. Comparisons of the results of the calculation technique employed with the available limited data, together with the agreement of this with previous estimates, lead us to suppose that a 60-percent channel-by-channel uncertainty is a reasonable estimate at this time.

The accuracy with which line features can be identified and removed from the spectrum depends on the total number of counts. To a good first approximation, the channel-by-channel variance will be twice the total number of raw counts in that channel. The total raw counts used in the Apollo-16 analysis were 11698, 10337, 4984, and 1150 for the energy bands of Table 2.

The uncertainties in the shielding and scattering effects are important at low energies where, as indicated in the previous section, they are estimated to be as large as 35 percent.

(d) Results

Figure 3 shows the residual continuum energy-loss spectrum for Apollo-16 after all background subtractions, and the standard deviation is indicated every 25 or 50 channels. In Figure 4, the equivalent photon spectrum is plotted within an envelope defining the one standard deviation error obtained as described above. This error envelope was constructed to smoothly enclose the largest error bars in any region. A similar analysis has been carried out for Apollo-15 and the same distribution and error band have been obtained. In order to

aid other investigators in comparing data, representative values are given in Table 3.

V. DETERMINATION OF FLUX ISOTROPY

A determination of the isotropy of the cosmic gamma-ray flux can be an extremely sensitive test of cosmological origin and, in addition, may provide a measure of the strength of galactic gamma-ray emission in the 0.3- to 10-MeV energy region. The transearth coast period of the Apollo mission provided an opportunity for a study of the astronomical sources of gamma radiation, using the opaque spacecraft and the anisotropic mass distribution of the instrument to occult possible source regions. For this purpose, the boom length was fixed at 2 m. As the spacecraft rotated at approximately three revolutions per hour for thermal control, various regions of the sky became occulted. Changing the spacecraft spin-axis direction caused the plane of occultation to vary. Preliminary results show a modulation of approximately five percent in the integral energy-loss spectrum up to 1 MeV, attributable to discrete sources primarily in the galactic plane. Once allowance is made for the levels of the various backgrounds, this modulation indicates that the equivalent cosmic photon spectrum shown in Figure 4 may have a contribution of approximately 20 percent from these galactic sources in the energy region up to 1 MeV. Statistically significant results for higher energies have not as yet been obtained.

VI. DISCUSSION

In Figure 4, comparison is made between the Apollo data and the latest data available for the 0.1- to 0.2-MeV and 30- to 100-MeV energy regions. The spectra can be seen to connect smoothly and there is some indication of a flatter slope in the 1- to 5-MeV region. However, the significance of such an excess component over a smooth power-law connection of low- and high-energy data is now only approximately 1.5σ .

In Figure 5, many sources of data for the 0.1- to 100-MeV energy range are presented. Where a particular experimental method or analysis has been repeated, only the latest estimates are given, except for the case of Apollo where the original estimate is included for comparison. As a greater realization of potential background problems develops, the data are tending to converge to a considerably lower estimate of the 1- to 20-MeV radiation. The particular difficulties in other techniques will not be discussed here, but the reader is referred to a recent review by Horstman et al. (1975) and recent papers by Schonfelder et al. (1975) and Daniel and Lavakare (1975).

There has been much interesting theoretical speculation concerning the shape of the diffuse cosmic gamma-ray spectrum. A single power-law spectrum would favor a single-source mechanism, for example, the Compton scattering of electrons on the 3 K background radiation (Felten and Morrison, 1963; Brecher and Morrison, 1969). At the same time, a significant excess in the 1- to 20-MeV region could indicate a component due to red-shifted π^0 -decay

resulting from cosmic-ray interactions (Stecker, 1969) or matter-antimatter annihilation (Stecker et al., 1971). The lowering of the 1- to 20-MeV estimates again makes a single-source mechanism possible.

Clearly, measurements must be made which will reduce the error bars across the entire spectrum and enable subtraction of point sources before definitive statements may be made as to whether the spectrum reflects more than one source mechanism. The analysis of the Apollo data suggests many improvements that can be made in the important region from 0.3 to 20 MeV. Heavy spacecraft produce a hard photon continuum and secondary neutrons which are difficult to shield against without compounding the problem. In the Apollo detectors, these effects were reduced by extension on a 7.6-m boom for long periods. For a crystal stowed in such a spacecraft, prompt neutron effects and short-lived induced radioactivity would make the neutron contribution far worse. Also, it can be seen that a very efficient anticoincidence shield against charged particles is required to perform measurements above 10 MeV, while unshielded materials are a source of bremsstrahlung. Many lines that are of potential cosmic importance can also be produced in materials that are commonly used in detector housing and spacecraft components. We believe that the most favorable signal-to-noise ratio for this spectral band can be achieved using a lightweight spacecraft in interplanetary space. Use of a particle anticoincidence mantle surrounding the entire spacecraft would remove all prompt effects and leave a cosmic gamma-ray signal about twice the level

produced by local activation due to cosmic rays. The latter component can be calculated, estimated from laboratory calibrations, and/or monitored in flight. Discrete gamma-ray line fluxes can be reduced by the careful selection and location of materials and angular distributions investigated using an anisotropic central crystal (Trombka et al., 1974).

VII. ACKNOWLEDGMENTS

C. S. Dyer wishes to acknowledge an NAS/NRC resident research association held during the majority of this work, and support at the University of Maryland under NASA Grant NGL-21-002-033. R. H. Parker, R. E. Parker, and E. MacMillan of the Jet Propulsion Laboratory (JPL) produced the mass-distribution profile of the gamma-ray spectrometer. D. Gilman at Cornell and R. H. Parker at JPL have been pursuing the analysis of the spacecraft occultation modes. A. E. Metzger is pleased to acknowledge a fruitful conversation with E. C. Stone of the California Institute of Technology (Caltech). Work at the Jet Propulsion Laboratory of the California Institute of Technology was carried out under NASA Contract NAS 7-100.

Table 1

Contribution of Discrete Lines

<u>Energy</u> <u>(MeV)</u>	<u>Intensity in Photons s⁻¹</u>	
	<u>Apollo-15</u>	<u>Apollo-16</u>
0.48 ± 0.02	0.91 ± 0.13	1.12 ± 0.10
0.51 ± 0.02	1.43 ± 0.14	1.87 ± 0.11
0.74 ± 0.03	0.32 ± 0.11	0.22 ± 0.08
0.84 ± 0.03	0.30 ± 0.11	0.28 ± 0.08
0.98 ± 0.03	0.14 ± 0.12	0.23 ± 0.09
1.31 ± 0.04	0.21 ± 0.17	0.29 ± 0.12
1.37 ± 0.04	0.36 ± 0.19	0.66 ± 0.13
1.46 ± 0.04	0.81 ± 0.16	0.72 ± 0.12
1.64 ± 0.05	0.48 ± 0.15	0.60 ± 0.12
1.78 ± 0.05	0.42 ± 0.15	0.57 ± 0.12
2.28 ± 0.06	0.09 ± 0.10	0.30 ± 0.13
2.75 ± 0.07	0.20 ± 0.09	0.28 ± 0.11
4.40 ± 0.08	0.19 ± 0.05	0.06 ± 0.07

Table 2

Composition of Apollo Spectrum (Percentage Contribution)

Energy (MeV)	Spacecraft		Brems- strah- lung		Neutron		Cosmic- ray		Discrete Lines		Cosmic	
	A15*	A16*	A15	A16	A15	A16	A15	A16	A15	A16	A15	A16
0.4- 0.8	18	15	12	19	12	11	12	11	15	16	31	27
0.8- 2.0	15	13	14	23	9	8	28	24	11	12	22	20
2.0- 5.0	20	17	19	30	6	5	33	29	3	3	19	17
5.0-10.0	40	33	26	42	0	0	11	10	0	0	23	16

*A15 - Apollo-15

A16 - Apollo-16

Table 3

Cosmic Gamma-Ray Continuum

<u>Energy</u> <u>(MeV)</u>	<u>Intensity</u> <u>(photons MeV⁻¹ cm⁻² s⁻¹ sr⁻¹)</u>
0.3	0.16 ± 0.06
0.4	0.067 ± 0.021
0.5	0.039 ± 0.012
0.6	0.027 ± 0.008
0.8	0.017 ± 0.005
1.0	0.013 ± 0.005
1.5	0.0080 ± 0.0038
2.0	0.0055 ± 0.0031
3.0	0.0025 ± 0.0013
4.0	0.0013 ± 0.0006
5.0	0.00070 ± 0.00028
6.0	0.00042 ± 0.00018
8.0	0.00018 ± 0.00011
10.0	0.000095 ± 0.000060

References

- Berger, M. J. and S. M. Seltzer, 1968, NASA SP-169, p. 285.
- Berger, M. J. and S. M. Seltzer, 1972, Nucl. Instr. and Methods, 104, p. 317.
- Bratolyuhova-Tsulukidze, L. I., N. L. Grigorov, L. F. Kalinkin, A. S. Melioransky, E. A. Pryakhin, I. A. Savenho, and V. Ya Yufarkin, 1971, Geomagnetism and Aeronomy (Soviet), 11, p. 585.
- Brecher, K. and P. Morrison, 1969, Phys. Rev. Lett., 23, p. 802.
- Daniel, R. R., G. Joseph, and P. J. Lavakare, 1972, Astrophys. and Space Sci., 18, p. 462.
- Daniel, R. R. and P. J. Lavakare, 1975, "Proceedings of the IUPAP 14th International Cosmic Ray Conference," 1, p. 23.
- Dennis, B. R., A. N. Suri, and K. J. Frost, 1973, Astrophys. J., 186, pp. 97-107.
- Dyer, C. S., A. R. Engel, and J. J. Quenby, 1972, Astrophys. and Space Sci., 19, p. 359.
- Dyer, C. S., J. I. Trombka, R. L. Schmadebeck, E. Eller, M. J. Bielefeld, G. D. O'Kelley, J. S. Eldridge, K. J. Northcutt, A. E. Metzger, R. C. Reedy, E. Schonfeld, S. M. Seltzer, J. R. Arnold, and L. E. Peterson, 1975a, Space Science Instrumentation, 1, pp. 279-288.
- Dyer, C. S., J. I. Trombka, A. E. Metzger, S. M. Seltzer, M. J. Bielefeld, and L. G. Evans, 1975b, "Proceedings of the IUPAP 14th International Cosmic Ray Conference," 1, p. 2.

Felten, J. E. and P. Morrison, 1963, Phys. Rev. Lett., 10, p. 453.

Fichtel, C. E., R. C. Hartman, D. A. Kniffen, D. J. Thompson, G. F.

Bignami, H. Ögelman, M. F. Özel, and T. Tümer, 1975, Astrophys. J.,
198, p. 163.

Fishman, G. J., 1972, Astrophys. J., 171, p. 163.

Fukuda, Y., S. Hayakawa, I. Kashara, F. Makino, Y. Tanaka, and B. V.

Sreekantan, 1975, Nature, 254, p. 398.

Hall, R. D., C. A. Meegan, G. D. Walraven, F. T. Djuth, D. H. Shelton,
and R. C. Haymes, 1975, "Proceedings of the IUPAP 14th International
Cosmic Ray Conference," 1, p. 84.

Harrington, T. M., J. H. Marshall, J. R. Arnold, L. E. Peterson, J. I.

Trombka, and A. E. Metzger, 1974, Nucl. Instr. and Methods, 118,
pp. 401-411.

Haymes, R. C., G. D. Walraven, C. A. Meegan, R. D. Hall, F. T. Djuth,
and D. H. Shelton, 1975, Astrophys. J., 201, p. 593.

Herterich, W., K. Pinkau, H. Rothermel, and M. Sommer, 1973, "Proceedings
of the IUPAP 13th International Cosmic Ray Conference," 1, p. 21.

Hopper, V. D., O. B. Mace, J. A. Thomas, P. Albats, G. M. Frye, Jr.,

G. B. Thomson, and J. A. Staib, 1973, Astrophys. J. Lett., 186, p. L55.

Horstman, H. M., G. Cavallo, and E. Moretti-Horstman, 1975, Rivista Del
Nuovo Cimento, 5, p. 255.

Horstman-Moretti, E., F. Fuligni, H. M. Horstman, and D. Brini, 1974,

Astrophys. and Space Sci., 27, p. 195.

Kuo, Fu-Shong, G. H. Frye, Jr., and A. D. Zych, 1973, Astrophys. J. Lett.,

186, p. L51.

Mazets, E. P., S. V. Golenetskii, V. N. Il'inski, Yu. A. Gur'yan, and

T. V. Kharitonova, 1975, Astrophys. and Space Sci., 33, p. 347.

Metzger, A. E. and J. I. Trombka, 1972, "Proceedings of the National Sym-

posium on Natural and Manmade Radiation in Space," Warman, E. A., ed.,

NASA TM X-2440.

Parlier, B., M. Forichon, T. Montmerle, B. Agrinier, G. Boella, L. Scarsi,

M. Niel, and R. Palmeira, 1975, "Proceedings of the IUPAP 14th Inter-

national Cosmic Ray Conference," 1, p. 14.

Schonfelder, V., G. Lichti, J. Daugherty, and C. Moyano, 1975, "Proceedings

of the IUPAP 14th International Cosmic Ray Conference," 1, p. 8.

Seltzer, S. M., 1975, Nucl. Instr. and Methods, 127, p. 293.

Seltzer, S. M., 1976, to be published.

Share, G. H., R. L. Kinzer, and N. Seeman, 1974, Astrophys. J., 187, p. 511.

Silberberg, R. and C. H. Tsao, 1973, Astrophys. J. Suppl., 25, p. 315.

Stecker, F. W., 1969, Nature, 224, p. 870.

Stecker, F. W., D. L. Morgan, and J. Bredekamp, 1971, Phys. Rev. Lett.,

27, p. 1469.

Teegarden, B. J., F. B. McDonald, J. H. Trainor, W. R. Webber, and

E. C. Roelof, 1974, J. Geophys. Res., 79, p. 3615.

Trombka, J. I. and R. L. Schmadebeck, 1968, NASA SP-3044.

Trombka, J. I., A. E. Metzger, J. R. Arnold, J. L. Matteson, R. C. Reedy,
and L. E. Peterson, 1973, Astrophys. J., 3(1), pp. 737-746.

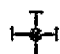
Trombka, J. I., J. I. Vette, F. W. Stecker, E. L. Eller, and W. T. Wildes,
1974, Nucl. Instr. and Methods, 117, p. 99.


Trombka, J. I., E. L. Eller, R. L. Schmadebeck, C. S. Dyer, R. C. Reedy,
D. W. Barr, J. S. Gilmore, R. L. Prestwood, B. P. Bayhurst, D. G.
Perry, A. E. Smith, R. C. Cordi, R. H. Pehl, J. S. Eldridge, E.
Schonfeld, and A. E. Metzger, 1976, ASTP Preliminary Science Report,
NASA TM X-58173.

Vedrenne, G., F. Albernhe, I. Martin, and R. Talon, 1971, Astr. and
Astrophys., 15, p. 50.

Figure Captions


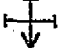






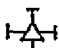



1. The total energy-loss spectra observed at full (7.6-m) boom extension on Apollo-15 and Apollo-16 are compared with the calculated levels of various backgrounds discussed in the text. The latter are shown for the Apollo-16 measurement. The only component to change significantly is the electron bremsstrahlung, which, at the time of Apollo-15, was approximately half the value shown.
2. The energy-loss spectrum (+) of the discrete line background for the Apollo-16 measurement is compared with the fitted line spectrum (solid line) obtained by the iterative unfolding procedure.
3. The energy-loss spectrum (points) of the cosmic gamma-ray component obtained after the subtraction of all backgrounds is compared with the energy-loss equivalent (solid line) of the unfolded photon spectrum. Error bars are plotted every 25 or 50 channels and include the effect of statistics and the uncertainties in the subtraction of backgrounds.
4. The unfolded photon spectrum from the Apollo data is shown by the line within the $\pm 1\sigma$ error band. Comparison is made with the recent high- and low-energy data. Hatched area is the SAS-2 Measurement (Fichtel et al., 1975):

 Dennis et al. (1973)

 Horstman-Moretti et al. (1974)

5. The diffuse cosmic gamma radiation observed by several experiments.

Some convergence of the data has occurred as awareness of spurious background has increased.

-  Hopper et al. (1973)
-  Bratolyubova-Tsulukidze et al. (1971)
-  Share et al. (1974)
-  Herterich et al. (1973)
-  Parlier et al. (1975)
-  Kuo et al. (1973)
-  Trombka et al. (1973), (earlier Apollo estimate)
-  Schonfelder et al. (1975)
-  Daniel et al. (1972) and Daniel and Lavakare (1975)
-  Vedrenne et al. (1971). For sake of clarity a typical error bar is shown for only one point.
-  Mazets et al. (1975)
-  Fukada et al. (1975)

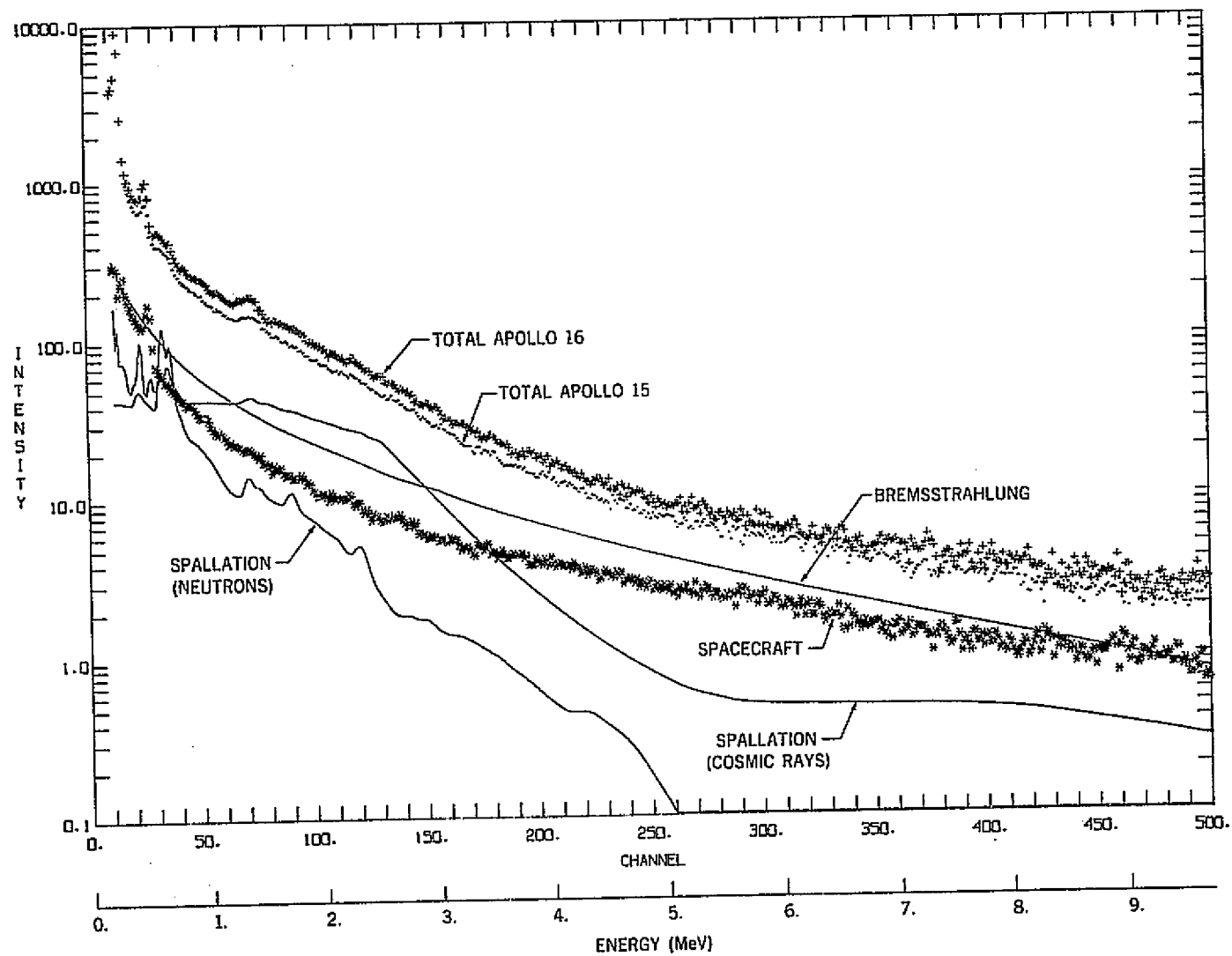


Fig. 1

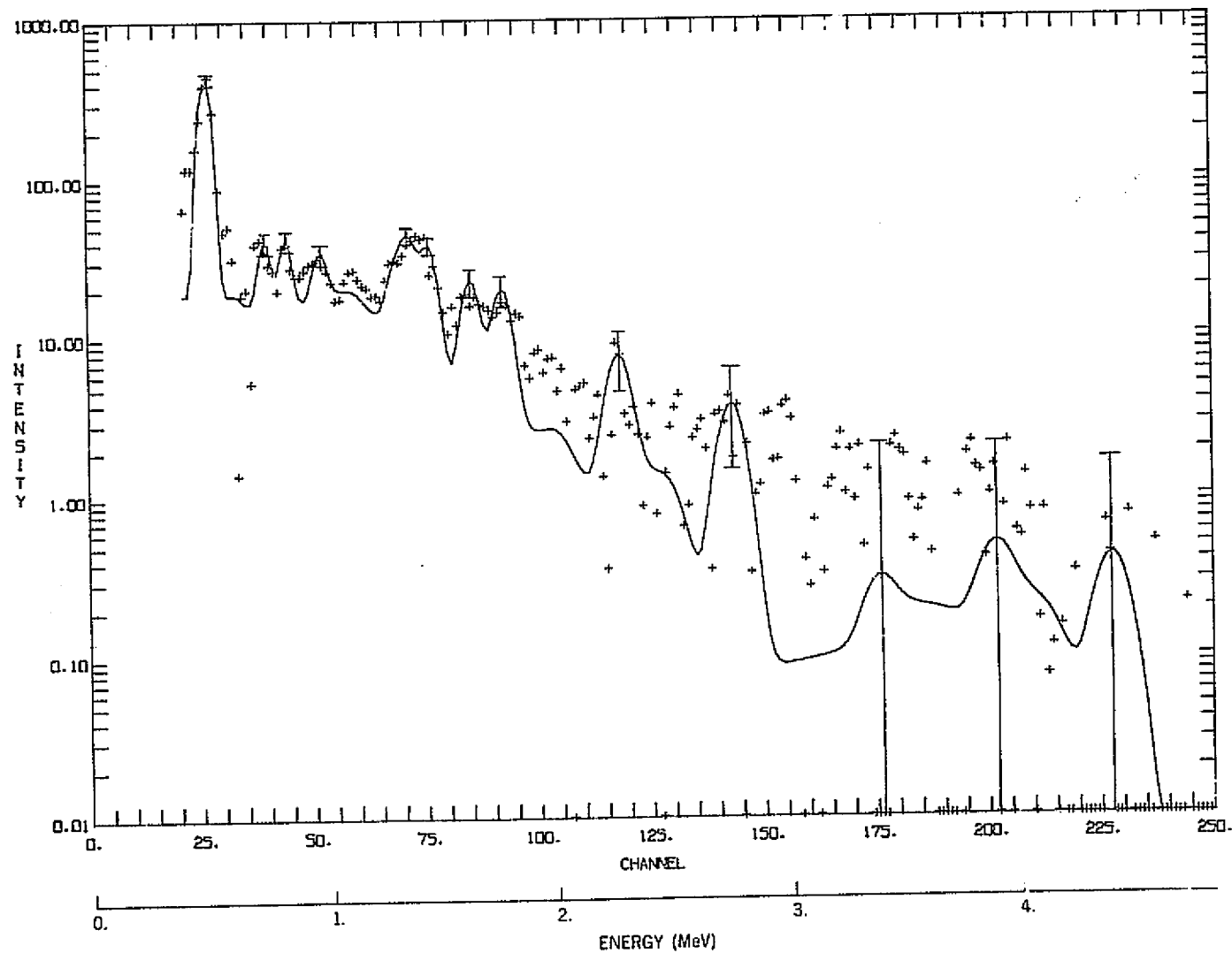


Fig. 2

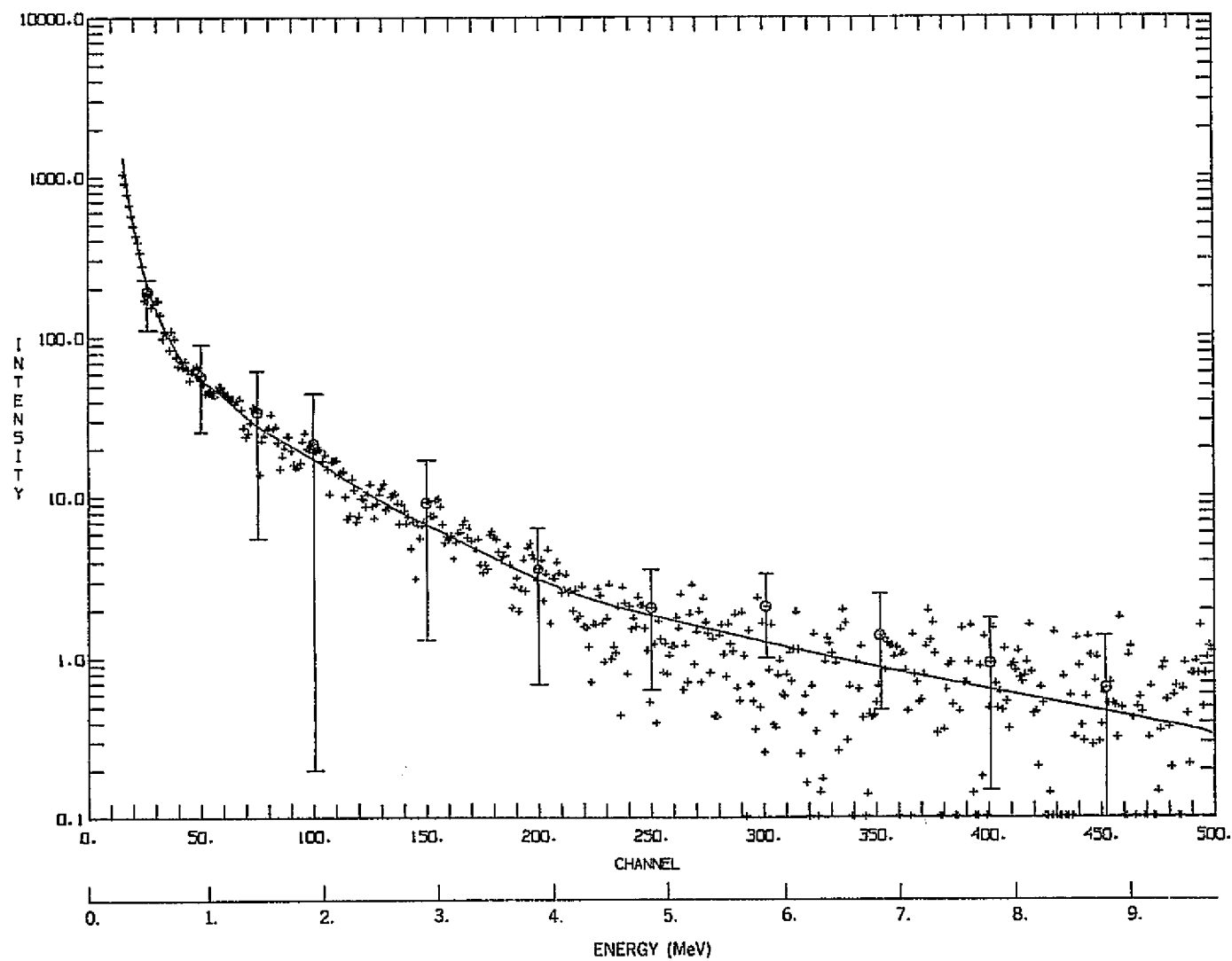


Fig. 3

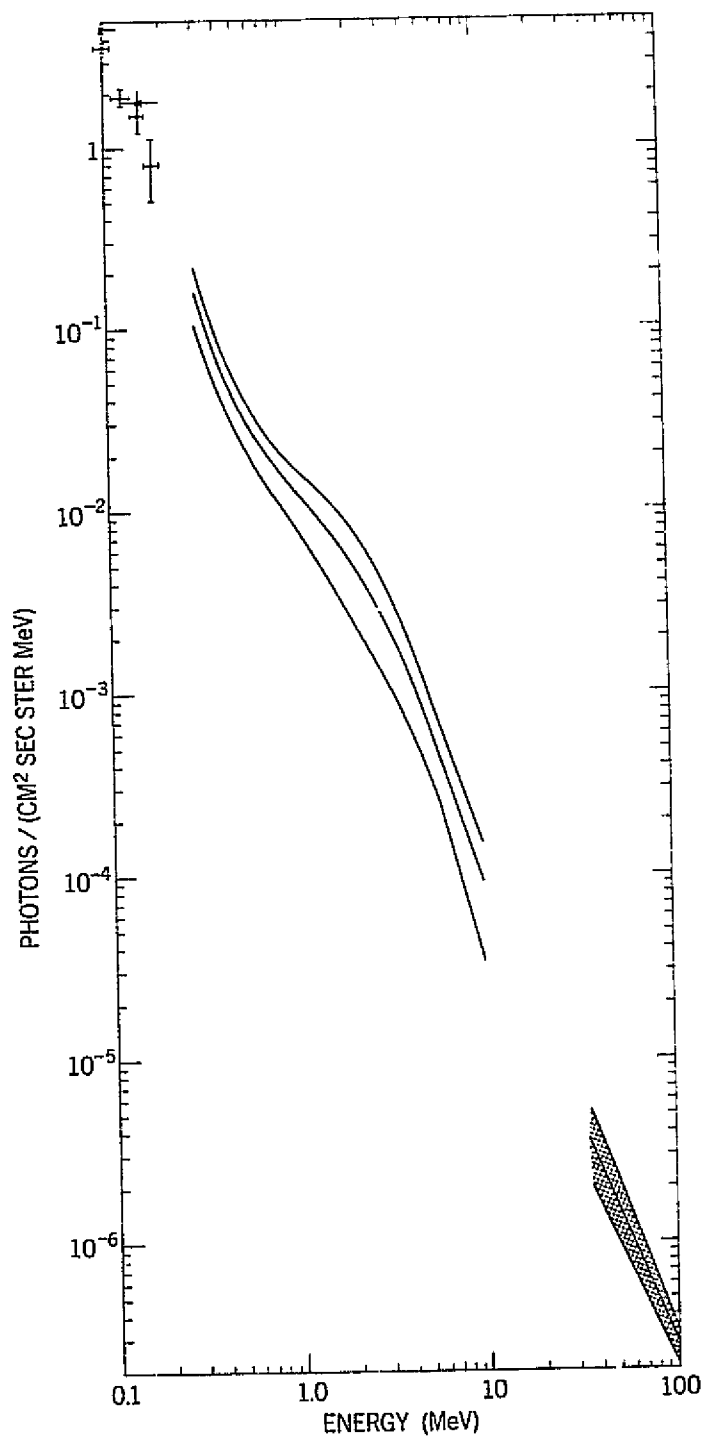


Fig. 4

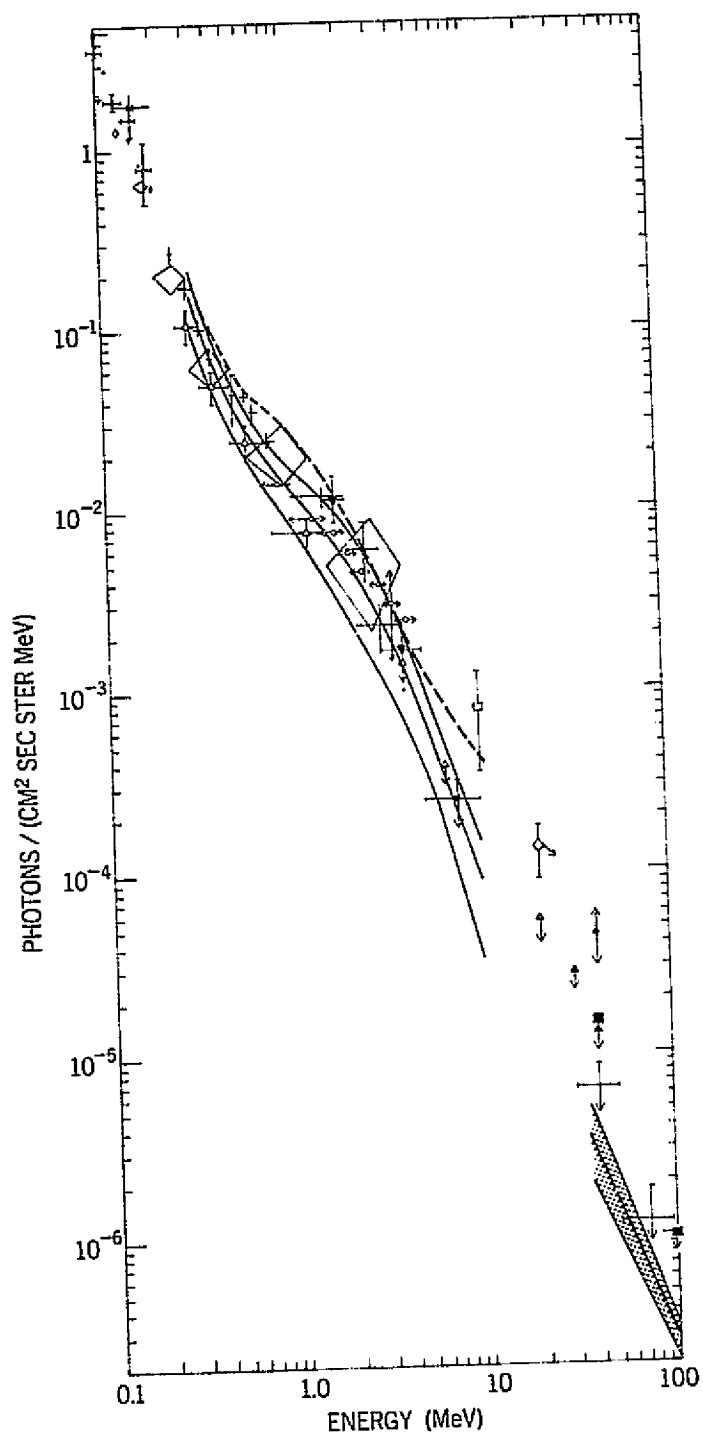


Fig. 5